Inequivalent atoms and imaging mechanisms in ac-mode atomic-force microscopy of Si(111)7×7

Ragnar Erlandsson, Lars Olsson, and Per Mårtensson
Laboratory of Applied Physics, Department of Physics and Measurement Technology, Linköping University, S-581 83 Linköping, Sweden
(Received 20 May 1996)

ac-mode atomic-force microscopy (AFM) has been used to image the Si(111)7×7 reconstruction. The corner holes and adatoms in the 7×7 unit cell as well as isolated atomic defects are clearly resolved. In addition, we observe a contrast between inequivalent adatoms, the center adatoms appearing 0.13 Å higher than the corner adatoms. We show that AFM does not image the true atom positions nor the charge density in the dangling bonds. Rather, our data suggest that the contrast is due to a variation in the chemical reactivity of the adatoms or to a tip-induced atomic-relaxation effect reflecting the stiffness of the surface lattice. [S0163-1829(96)50536-9]

Since the invention of the atomic-force microscope (AFM) in 1986,[1] a considerable effort has been devoted to develop the technique to a point that would allow routine investigation of atomic structure as has been possible using scanning tunneling microscopy (STM) (Ref. 2) for more than a decade. The development of AFM has, however, been disappointingly slow for investigations of well-characterized surfaces in ultrahigh vacuum (UHV). One reason for this is that the long-range attractive force acting over a large part of a tip in contact with a surface will cause a repulsive force at the foremost apex atom which is difficult to control.[3] This force can easily exceed the limit where the integrity of the sample and tip is destroyed ($\sim 1\times 10^{-9}$ N),[4] making true atomic-resolution imaging impossible.

The AFM can be operated in several different operating modes.[3] We distinguish between contact mode (cm) and noncontact mode depending on if the tip apex enters the repulsive part of the potential or not, and ac and dc mode depending on if the cantilever is oscillated or not. Of the various AFM modes, the problem due to long-range attraction is most severe in the dc contact mode where the tip is in repulsive contact with the sample during the entire imaging process. Therefore, it is in many cases unclear if dc-cm images showing atomic corrugation for layered[5] as well as nonlayered materials[3] actually represent individual atoms or if the contrast is due to friction and/or collective effects involving many atoms in the contact area. Contact mode images that fulfill the most stringent definition of atomic resolution, i.e., showing isolated defects or sharp steps in addition to atomic corrugation, have to our knowledge only been presented in two cases. Giessibl and Binnig[6] have observed a sharp step in an image of KBr obtained in UHV at 4 K and Ohnesorge and Binnig[7] have observed isolated defects in a calcite surface when operating the AFM in liquid. A breakthrough in AFM imaging was the recent demonstration by Giessibl,[8] Kitamura and Iwatsuki,[9] and Ueyama *et al.*[10] that ac-mode force microscopy can give true atomic resolution. When the AFM is used in this mode the problems associated with long-range attractive forces are reduced since the tip moves in and out of the interaction region during the oscillation around the equilibrium position.

We have used ac-mode AFM to image the Si(111)7×7 reconstruction, described by the dimer-adatom-stacking fault (DAS) model[11] (see Fig. 1). Previous AFM studies of this surface have resolved the 7×7 unit cell and the individual adatoms.[8,9,12,13] We observe, in addition, a contrast between the inequivalent adatoms and discuss the origin of this effect.

The Si(111)7×7 surfaces were prepared by heat treatment[14,15] of samples cut from a highly *n*-doped Si(111) wafer. The AFM image in Fig. 2 was obtained using a home-built combined AFM/STM operating in UHV.[14] For AFM imaging, we operate the instrument in the ac mode: the cantilever is oscillated at the resonance frequency and the tip to sample separation is regulated in order to obtain a constant reduction in oscillation amplitude. The cantilever/tip units, made from etched tungsten wires, were heat cleaned *in situ* using electron bombardment. The cantilever/tip used to acquire the AFM image shown in Fig. 2(a) had a resonance frequency of 16.4 kHz, a quality factor of 550, a tip radius estimated to <150 Å from scanning electron microscopy data, and a spring constant of approximately 60 N/m as estimated from the cantilever geometry. The quality factor of our tungsten cantilever with circular cross section is approxi-

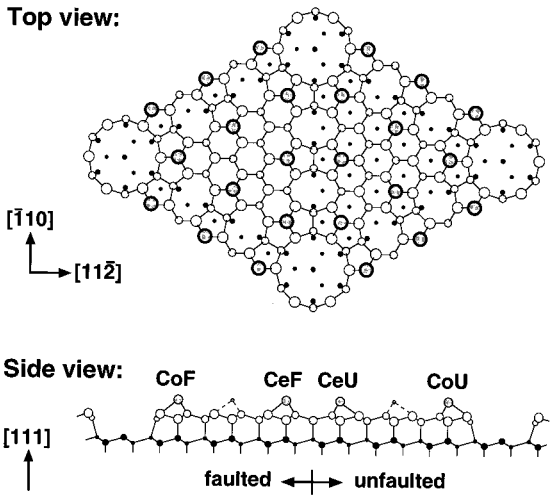

FIG. 1. Top and side views of the Si(111)7×7 reconstruction as described by the DAS model. The adatoms occupy four equivalent sites denoted: CoF, corner faulted; CeF, center faulted; CeU, center unfaulted; and CoU, corner unfaulted.

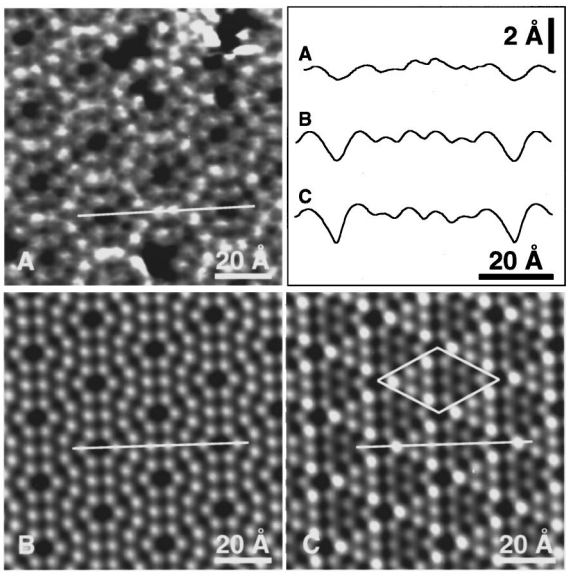

FIG. 2. A comparison between (a) an AFM image and (b) empty- and (c) filled-state STM images. The grey scales in the images correspond to a height difference of 1 Å . The STM images were recorded with tip voltages of -2 and $+2.2$ V, respectively, and a constant current of 0.1 nA. The AFM image has been low-pass filtered using a 3×3 convolution filter while the STM images show unfiltered data. The cross sections through the four inequivalent adatoms are obtained from raw data. The 7×7 unit cell is outlined in the filled-state STM image. The faulted and unfaulted halves correspond to the left-hand and right-hand side, respectively.

mately the same in air and vacuum and has a significantly lower value than those reported for the silicon cantilevers used by others.[8–10,13,16] The STM images in Fig. 2 were acquired using a conventional homebuilt UHV STM and etched tungsten tips cleaned by electron-bombardment heating.[15]

In Fig. 2, we show a comparison between an AFM image and a pair of dual-polarity STM images showing the Si(111)7×7 reconstruction. Although both the AFM and STM images show the positions of the adatoms, there is an additional contrast between the nonequivalent corner and center adatoms in the AFM data (see Figs. 1 and 2). This is, to our knowledge, the first time that inequivalent atoms of the same species have been distinguished by their contrast in an AFM image. The possibility that the observed contrast is due to a geometric tip effect can be excluded, since the apparent height of a center adatom is the same whether it is located adjacent to a vacancy or not. We have also observed the same contrast in several images for which stochastic tip changes have occurred in between, such that the cluster of the foremost tip atoms has been different for the different images. As is shown by Pérez *et al.*,[17] the presence of a dangling bond on the apex atom directed towards the surface is expected to have a dramatic effect on the observed contrast. We have, however, no way of determining whether this atom is a tungsten, oxygen, or silicon species. We find that AFM imaging is more prone to stochastic tip events than STM imaging. Additionally, we observe a stronger tendency for tip-induced contamination during AFM imaging as compared to STM, despite the tip cleaning by electron-bombardment heating.

In Fig. 2 we also show a cross section through the raw data along the long diagonal of the 7×7 unit cell. This cross section shows the tip trace above the corner holes and the four inequivalent adatoms, allowing the comparison of the contrast observed in the AFM image with the well-known contrast in filled- and empty-state STM images.[18] In the empty-state STM image there is no contrast between the faulted and unfaulted halves of the unit cell and all 12 adatoms appear identical. Imaging filled states, the corner adatoms appear slightly higher as compared to the adjacent center adatoms and the faulted halves of the unit cell appear slightly higher than the unfaulted halves. The depth of the corner holes in the AFM data (~1 Å) is smaller than the depth observed in the filled- and empty-states STM images (~2 Å). In the cross section of the AFM image, the difference in apparent height of the corner and center adatoms is clearly seen. When averaged over several unit cells, the height difference was determined to 0.13 Å. Although there is no contrast between the inequivalent halves of the unit cell in the AFM image in Fig. 2, a weak contrast has been observed in other less well-resolved images. That the fine details of the contrast can vary between images is not too surprising in view of the relatively frequent tip changes taking place during data acquisition, most likely resulting in variations of the detailed atomic structure of the tip apex.

In order to correlate the AFM contrast to quantitative details of atomic-scale electronic and structural properties of the surface, it is of crucial importance to understand the ac-mode imaging process.[19] Some insight can be obtained by studying approach curves showing the cantilever deflection (force) and the resonance amplitude as a function of sample position, see Fig. 3(a). In these approach curves, recorded after acquiring the image presented in Fig. 2(a), it can be seen that the oscillation amplitude (initially 16 $Å_{p-p}$) starts to decrease some 30 Å before the sudden attractive response in the cantilever deflection curve (snap-in) after which the cantilever oscillation is completely damped. On retraction, the tip sticks to the sample until it is pulled back ~9 Å from the snap-in point. When this occurs there is a sudden rise in the amplitude, after which the curve follows the same trace as the ingoing curve.

To clarify the mechanism behind the observed damping, we record the frequency spectra of the cantilever as a function of sample position, see Fig. 3(b). After obtaining a small force-induced frequency shift (curve 2), the sample is moved toward the tip in 3-Å steps. Two distinct mechanisms that lead to an amplitude decrease for a constant driving frequency can be distinguished, a pure shift of the resonance frequency and damping related to energy loss. Initially, the curve shifts due to the long-range attractive force, which is a combination of the van der Waals interaction and the electrostatic force due to the contact potential (as no external bias voltage was applied, the potential between tip and sample is given by the difference in work function, which is estimated to be <0.5 V). For separations corresponding to curves 2 and 3, there is no significant damping of the oscillation. Between curves 3 and 4, the tip comes in repulsive contact with the surface as can be seen from the truncated shape of curve 4. After this, both the amplitude and the resonance frequency of the cantilever continue to decrease. The behavior of the frequency spectra during sample approach is consistent with

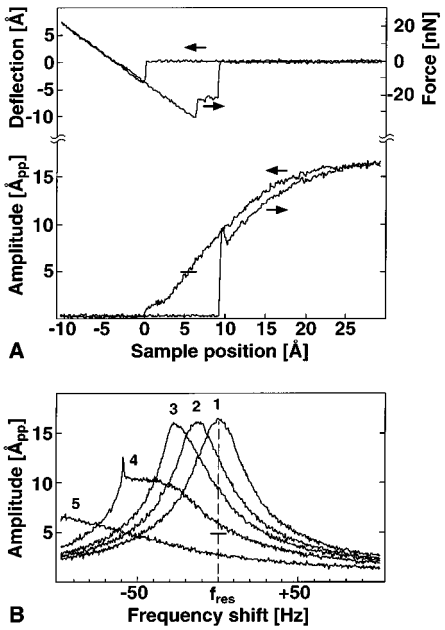

FIG. 3. (a) The deflection of the cantilever (upper curve) and the peak-to-peak oscillation amplitude (lower curve) as a function of sample position. The zero on the horizontal axis is defined as the point of initial hard contact and negative numbers correspond to contact. The force scale only gives approximate values as the spring constant of the cantilever is not precisely known. The applied oscillation in the cantilever-deflection signal is not seen since it was low-pass filtered with a cutoff frequency of 100 Hz. The horizontal bar intersecting the amplitude curve indicates the operating point (5 Å). (b) A series of resonance spectra of the cantilever for different tip-to-sample separations. Curve 1 was recorded at a separation where no force was detected, giving the resonance frequency of the undisturbed oscillation. Curves 2–5 were recorded for sample positions corresponding to 12, 15, 18, and 21 Å with respect to curve 1, moving the sample towards the tip. The horizontal scale shows the deviation from the undisturbed resonance frequency. The horizontal bar intersecting the line showing the undisturbed resonance frequency indicates the operating point (5 Å).

the amplitude curve in Fig. 3(a). It should be noted that it is impossible to distinguish between the two mechanisms affecting the frequency spectra from the amplitude curve alone since the transition from a frequency shift to a contact-induced damping does not give any signature. The AFM image shown in Fig. 2(a) was recorded for a constant reduced amplitude of 5 Å$_{p-p}$ as compared to the 16-Å$_{p-p}$ free amplitude. The data in Fig. 3 strongly suggest that we operate with the tip entering the repulsive part of the potential during the oscillation cycle. Previous atomically resolved ac-mode measurements[8–10,13] have obtained the regulation signal using a frequency modulation technique that, at least ideally, should respond only to the frequency shift. A detailed description of how this frequency shift varies with tip-to-sample separation is given by Lüthi *et al.*[16]

The key question raised by the results presented here is the origin of the atomic contrast observed for the Si(111)7×7 reconstruction. Ciraci, Baratoff, and Batra[20] have shown that the force between the tip and the sample in atomic-force microscopy can be divided into two terms, one originating from the Coulomb repulsion between the ion cores F_{ion}, and another that is due to the interaction of the valence electrons with the ion cores F_{el}. For small tip-surface separations, F_{ion} is dominating such that the AFM to the first approximation is probing the position of the ion cores when operated in the close contact regime. At larger separations, F_{el} will dominate due to the rapid decay of F_{ion} and the AFM contrast is expected to reflect the total charge density of the sample. The Si(111)7×7 surface has been extensively studied, both experimentally and theoretically, and the exact position of the atom cores as well as the charge in the dangling bonds of the four inequivalent adatoms are well known.[21,22] The corner adatoms have more charge than the center adatoms and there is more charge on the adatoms in the faulted half of the unit cell as compared to those in the unfaulted half. This is the origin of the contrast observed in filled-state STM images of the surface. Moreover, the vertical position of the adatom cores is directly related to the charge in the dangling bonds such that the adatoms with the most charge are located farther away from the surface. However, the height difference between the inequivalent adatoms would correspond to a much smaller contrast than that observed in the filled-state STM image (see Table I). From Fig. 2 and Table I, it is obvious that the observed AFM contrast neither represents the true ion core positions, nor the charge density in the dangling bond states (the AFM contrast is reversed compared to what would be expected if it reflected these properties).

TABLE I. Comparison between theoretically calculated (Ref. 21) relative vertical positions of the inequivalent adatoms and values obtained from filled-state STM data (tip voltage + 2.2 V and tunneling current 0.1 nA) and AFM data. All values are referred to the center adatom in the unfaulted half of the unit cell.

	Calculated position (Å)	STM filled states (Å)	AFM (Å)
CoF	0.085	0.53	−0.13
CeF	0.031	0.25	0.0
CeU	0.000	0.00	0.0
CoU	0.038	0.15	−0.13

A possible origin of the observed contrast could be variations in the relaxation of the outermost surface atoms due to the finite force between tip and sample during the small fraction of the oscillation cycle when the tip is in contact with the surface. Atomic-relaxation effects can be expected since interatomic spring constants are roughly of the order 10 N/m, i.e., they have a stiffness comparable to the cantilever used here.[7] This is supported by theoretical calculations for the Si(100)2×1 surface where large force-induced relaxation was observed,[4] but no such calculations have been presented for the Si(111)7×7 surface. Stich, Terakura, and Larson have recently performed an *ab initio* calculation of the dynamical properties of the Si(111)7×7 surface and determined the out-of-plane vibration frequencies of the inequivalent adatoms.[23] The center adatoms have higher frequencies (stiffer bonds) than the corner adatoms, in agreement with the AFM contrast, but the calculated difference between the vibration frequencies of adatoms in the faulted and unfaulted half of the unit cell is not consistent with our AFM data. However, it is unclear how well vibrational frequencies that

are related to individual bonds describe the relaxation due to an applied force which might cause a distortion of several bonds.

Another property of the surface atoms that could contribute to the contrast in AFM images is the chemical reactivity since the tip-apex atom is likely to form a bond with a surface atom during each oscillation cycle. If the making and breaking of a bond is associated with energy dissipation, a higher reactivity will result in a decrease of the cantilever resonance amplitude and thus a positive contrast. Chemical reactivity is clearly not a well-defined property of the surface atoms themselves as it also depends on the reacting species.[24] In several of the cases studied experimentally the trend is, however, that the center adatoms are more reactive than the corner adatoms,[25–30] in agreement with the AFM contrast we observe here. A similar trend has been observed for field evaporation extraction probabilities,[31] suggested to be related to the enhanced chemical reactivity of the center adatoms relative to the corner adatoms.

To determine whether a surface relaxation model or an argument involving chemical reactivity of the atoms is the best explanation of the contrast observed for the $Si(111)7\times7$ surface is premature at this stage, and would require theoretical calculations specifically addressing these issues. We hope, however, that the present demonstration of the capability of ac-mode AFM to image force-related properties on an atomic scale will stimulate theoretical efforts that will lead to a better understanding of the ac-mode imaging mechanism and establish a quantitative relationship between image contrast, cantilever dynamics, and atomic properties.

The authors would like to acknowledge the helpful discussions with Ingemar Lundström, Fredrik Owman, and Roger Wigren. The AFM activity at Linköping University was supported by the Swedish Research Council for Engineering Sciences (TFR).

[1] G. Binnig, C. F. Quate, and Ch. Gerber, Phys. Rev. Lett. **56**, 930 (1986).
[2] G. Binnig, H. Rohrer, Ch. Gerber, and H. Weibel, Phys. Rev. Lett. **49**, 57 (1982).
[3] F. J. Giessibl, Jpn. J. Appl. Phys. **33**, 3726 (1994).
[4] F. F. Abraham, I. P. Batra, and S. Ciraci, Phys. Rev. Lett. **60**, 1314 (1988).
[5] H. Heinzelmann, E. Meyer, D. Brodbeck, G. Overney, and H.-J. Güntherodt, Z. Phys. B **88**, 321 (1992).
[6] F. J. Giessibl and G. Binnig, Ultramicroscopy **42-44**, 281 (1992); G. Binnig, *ibid.* **42-44**, 7 (1992).
[7] F. Ohnesorge and G. Binnig, Science **260**, 1451 (1993).
[8] F. J. Giessibl, Science **267**, 68 (1995).
[9] S. Kitamura and M. Iwatsuki, Jpn. J. Appl. Phys. **34**, L145 (1995).
[10] H. Ueyama, M. Ohta, Y. Sugawara, and S. Morita, Jpn. J. Appl. Phys. **34**, L1086 (1995).
[11] K. Takayanagi, Y. Tanishiro, M. Takahashi, and S. Takahashi, J. Vac. Sci. Technol. A **3**, 1502 (1985).
[12] L. Howald, R. Lüthi, E. Meyer, and H.-J. Günterherodt, Phys. Rev. B **51**, 5484 (1995).
[13] P. Güthner, J. Vac. Sci. Technol. B (to be published).
[14] L. Olsson, R. Wigren, and R. Erlandsson, Rev. Sci. Instrum. **67**, 2289 (1996).
[15] F. Owman and P. Mårtensson, Surf. Sci. **324**, 211 (1995).
[16] R. Lüthi, E. Meyer, M. Bammerlin, A. Baratoff, T. Lehmann, L. Howald, Ch. Gerber, and H.-J. Güntherodt, Z. Phys. B **100**, 165 (1996).
[17] R. Pérez, M. C. Payne, I. Stich, and K. Terakura (unpublished).
[18] R. J. Hamers, R. M. Tromp, and J. E. Demuth, Phys. Rev. Lett. **56**, 1972 (1986).
[19] J. P. Spatz, S. Shekio, M. Möller, R. G. Winkler, P. Reineker, and O. Marti, Nanotechnology **6**, 40 (1995).
[20] S. Ciraci, A. Baratoff, and I. P. Batra, Phys. Rev. B **41**, 2763 (1990).
[21] K. D. Brommer, M. Needels, B. E. Larson, and J. D. Joannopoulos, Phys. Rev. Lett. **68**, 1355 (1992); K. D. Brommer, B. E. Larson, M. Needels, and J. D. Joannopoulos, Jpn. J. Appl. Phys. **32**, 1360 (1993).
[22] I. Stich, M. C. Payne, R. D. King-Smith, J.-S. Lin, and L. J. Clarke, Phys. Rev. Lett. **68**, 1351 (1992).
[23] I. Stich, K. Terakura, and B. E. Larson, Phys. Rev. Lett. **74**, 4491 (1995).
[24] K. D. Brommer, M. Galván, A. Dal Pino, Jr., and J. D. Joannopoulos, Surf. Sci. **314**, 57 (1994).
[25] St. Tosch and H. Neddermeyer, J. Microsc. **152**, 415 (1988).
[26] R. Wolkow and Ph. Avouris, Phys. Rev. Lett. **60**, 1049 (1988).
[27] J. Yoshinobu, D. Fukushi, M. Uda, E. Nomura, and M. Aono, Phys. Rev. B **46**, 9520 (1992).
[28] K. Uesugi, T. Takiguchi, M. Yoshimura, and T. Yao, J. Vac. Sci. Technol. B **12**, 2008 (1994).
[29] M. Shimomura, N. Sanada, Y. Fukuda, and P. J. Moller, Surf. Sci. **341**, L1061 (1995).
[30] J. A. Jensen, C. Yan, and A. C. Kummel, Phys. Rev. Lett. **76**, 1388 (1996).
[31] H. Uchida, D. Huang, F. Grey, and M. Aono, Phys. Rev. Lett. **70**, 2040 (1993).